FISEVIER

Contents lists available at ScienceDirect

# Journal of Theoretical Biology

journal homepage: www.elsevier.com/locate/yjtbi





# Cooperative SIR dynamics as a model for spontaneous blood clot initiation Philip Greulich\*

School of Mathematical Sciences, University of Southampton, Southampton, SO17 1BJ, United Kingdom Institute for Life Sciences, University of Southampton, Southampton, SO17 1BJ, United Kingdom

#### ARTICLE INFO

Dataset link: https://github.com/philipgreulich/cooperative-SIR

Keywords:
Blood clotting
Heterogeneity
SIR model
Collective phenomena

#### ABSTRACT

Blood clotting is an important physiological process to suppress bleeding upon injury, but when it occurs inadvertently, it can cause thrombosis, which can lead to life threatening conditions. Hence, understanding the microscopic mechanistic factors for inadvertent, spontaneous blood clotting, in absence of a vessel breach, can help in predicting and averting such conditions. Here, we present a minimal model – reminiscent of the SIR model – for the initiating stage of spontaneous blood clotting, the collective activation of blood platelets. This model predicts that in the presence of very small initial activation signals, collective activation of the platelet population is possible, but requires a sufficient degree of heterogeneity of platelet sensitivity. To propagate the activation signal and achieve collective activation of the bulk platelet population, it requires the presence of, possibly only few, hyper-sensitive platelets, but also a sufficient proportion of platelets with intermediate, yet higher-than-average sensitivity. A comparison with experimental results demonstrates a qualitative agreement for high platelet signalling activity.

#### 1. Introduction

Blood clotting is the formation of macroscopic aggregates of blood platelets which are stabilised by a fibrin polymer network (coagulation) (Gale, 2011). The physiological purpose of such an aggregate, called a blood clot, or thrombus, is to seal breached vessels and to protect an individual from blood loss. However, when blood clots emerge in the blood stream, away from vessel breaches, they can occlude vessels (thrombosis) and obstruct blood flow, which is associated with pathologies such as stroke and heart attacks (Raskob et al., 2014), leading to more than 15 million deaths per annum world-wide (British Heart Foundation, 2021).

The first stage of platelet-mediated blood clotting (*primary hemostasis*) is the formation of a *platelet plug* through platelet aggregation (Gale, 2011). Platelets can only aggregate once they have been activated. Activation is mediated by agonists in the bloodstream and vessel walls (usually arising from damaged vasculature), or through shear stresses and collisions with the vessel wall (Rana et al., 2019; Hellmuth et al., 2016), or indirectly, via paracrine signalling from other activated platelets (Stalker et al., 2012; van der Meijden and Heemskerk, 2019).

Physiological blood clotting occurs at vessel breaches, but blood clots can sometimes emerge without apparent vascular damage and with stimulant levels far below threshold levels expected to activate platelets (hypercoagulation) (LaPelusa and Dave, 2023). Although genetic and lifestyle risk factors for this are well established, the microscopic mechanistic origin of the emergence of such spontaneous blood

clotting (without apparent external activator) has so far eluded our full understanding.

It has been shown that platelets are highly diverse, and their sensitivity – the threshold and propensity to activate when exposed to stimulating factors – differs greatly between platelets within a person (van der Meijden and Heemskerk, 2019; Heemskerk and West, 2022; Jongen et al., 2020). Some platelets are extremely sensitive (Baaten et al., 2017), and it has been hypothesised that activation of such hypersensitive platelets – which might be rare, but can activate at very low stimulant concentrations – can propagate activation via paracrine signalling to activate also less sensitive platelets, thereby generating a macroscopic population of activated platelets. This could initiate platelet aggregation in situations where the abundance of stimulants is much lower than the threshold for the bulk activation of platelets (Baaten et al., 2017; Jongen et al., 2020; Lesyk and Jurasz, 2019). Thus, the diversity of platelet sensitivity, and not bulk platelet sensitivity alone, may drive platelet aggregation.

Platelet aggregation is measured by platelet aggregometry (Ruf et al., 1997), which employs several methods: the traditional "gold standard" is *light transmission aggregometry* (Born, 1962) which identifies platelet aggregation in an activated platelet suspension through increased light transmissibility. However, this method requires large sample volumes, long processing times and complex sample preparation (Koltai et al., 2017). Newer methods that measure impedance (Cardinal and Flower,

<sup>\*</sup> Correspondence to: School of Mathematical Sciences, University of Southampton, Southampton, SO17 1BJ, United Kingdom. E-mail address: P.S.Greulich@soton.ac.uk.

1980) and elastic properties (Thromboelastography, TEG) (Donahue and Otto, 2005) can also be performed on whole blood samples, and can measure whole blood clotting (TEG), not only aggregation. Flow cytometry uses fluorescent markers to measure activated platelets (Carubbi et al., 2014; Jongen et al., 2020) and thus can be used identify large scale platelet activation.

Whether activated clusters remain microscopic or the activation signal percolates through the platelet population, leading to collective activation/aggregation, is a non-trivial critical emergent phenomenon which has not been understood yet. Although models for blood clot growth have been widely used, those established models usually model blood clot growth at the vessel wall, from which strong activation stimulants are seccreted and where shear flow can trigger activation (Fogelson, 1993; Wang and Fogelson, 1999; Anand et al., 2003; Pivkin et al., 2006; Xu et al., 2008; Fogelson and Neeves, 2015; Fogelson, 2016; Schoeman et al., 2017; Link et al., 2020). How macroscopic platelet populations can get activated away from the vessel wall, when activation signals are absent or very low, is less understood.

In this work, we present a minimal mechanistic model for paracrine (platelet-platelet) activation via signalling, which captures the main qualitative features of the first phase of spontaneous blood clotting the macroscopic, collective activation of a platelet population, upon a weak stimulant signal, which usually would not be able to activate the bulk population of platelets alone. We thus propose a reactionrate model which can be translated into a dynamical system for the concentration of activated and naive platelets. This system has similarities to the SIR model, a model for the spread of infectious diseases (contagions), with the difference that multiple contagion-carrying agents (here: stimulant-secreting activated platelets) need to meet close to each other to spread the contagion (here: activation signal). We will show that even minor stimulation can lead to macroscopic activation of the platelet population away from vessel walls - which from a medical point of view can lead to a dangerous thrombus that occludes otherwise undamaged vessels - if there is a substantial degree of heterogeneity of platelet sensitivity.

#### 2. Model

Our aim is to model the transition from a naive, non-activated population of platelets, which are not able to aggregate, to a situation where a substantial proportion of the platelet population is activated. Activated platelets can adhere to each other, which is the pre-requisite for the first stage of blood clotting, platelet aggregation. To develop a thorough theoretical understanding we keep this model simple, by focusing only on the initiating step of platelet aggregation, the macroscopic activation of platelets, as further steps of blood clotting, platelet aggregation and coagulation, have been modelled elsewhere.

#### 2.1. Model assumptions

We make the following simplifying, yet biologically motivated assumptions:

- The platelet population is approximated as being *well mixed*, that is, each platelet can get in contact with each other platelet (the impact of this approximation is discussed in Section 4).
- Naive, non-activated platelets (N) can be activated either by external stimuli (e.g. activating agonists, shear flow stress, collisions), or by paracrine signalling (e.g. ADP) from other platelets in their immediate vicinity. A threshold amount of signalling molecules is required at their surface to activate (van der Meijden and Heemskerk, 2019; Jongen et al., 2020), as illustrated in Fig. 1.
- Freshly activated platelets  $(A_s)$  secret signalling molecules (e.g. ADP) which can activate other platelets ("degranulation") (van der Meijden and Heemskerk, 2019).

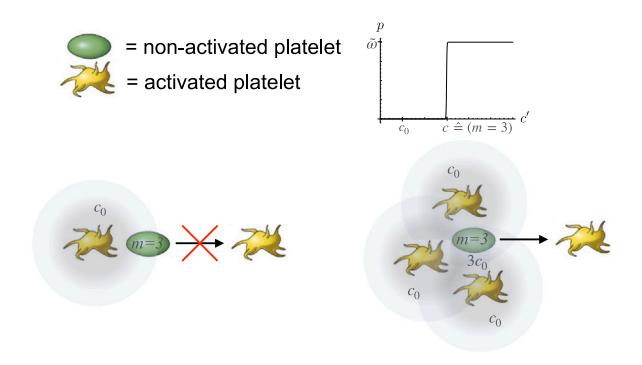


**Fig. 1.** Illustration of the model for the case  $c=3c_0$ , meaning m=3. (Top right:) The propensity p of a platelet to activate as function of the provided stimulant concentration c' for  $c=3c_0$  ( $\bar{\omega}$  is the maximal activation rate.). Only if  $c'\geq c$ , platelets can activate. (Bottom:) Illustration of the cooperative activation of platelets. A single secreting activated platelet provides only a stimulant level  $c_0$ , not sufficient to activate other naive platelets. However, if 3 secreting platelets are close to a naive platelet, their stimulants add linearly to provide  $c'=3c_0=c$ , which is sufficient to activate the naive platelet.

- Signalling molecules disperse quickly through diffusion and advection. Hence, the range of the signalling interaction is very short, and can be characterised by a stimulant concentration c<sub>0</sub> added by each activated secreting platelet, A<sub>s</sub>, to its immediate environment.
- The threshold amount of stimulus required to activate a naive platelet, c, might be higher than c<sub>0</sub>, the concentration provided by a single neighbouring secreting platelet.
- Degranulation occurs for a limited amount of time (Polasek, 2006), after which platelets turn into an idle activated state  $(A_i)$ , that is, they remain activated (and thus able to aggregate and initiate coagulation), but stop secreting activation signals.

These assumptions aim to simplify the model sufficiently to allow a thorough theoretical understanding, yet to retain the relevant features how paracrine signalling can spread the activation signal. This way, the model is expected to reproduce the qualitative features of macroscopic activation, e.g. to decide whether a transition from a microscopic to a macroscopic population of activated platelets is possible, and whether it occurs at a particular critical point of parameter values as an abrupt transition. The model is not intended to reflect a particular experimental situation and due to its approximative nature, it is not expected to reproduce accurate numerical predictions for experiments. However, it is expected to approximately model situations in which platelet activation (and possibly aggregation) occurs where platelets are immersed in blood flow, i.e. not bound to vessel walls, or in vitro situations where there is no flow.

# 2.2. Model for homogeneous platelet population

From these assumptions, we can formalise the activation dynamics of platelets. Let us assume that initially some, but not all platelets have been activated through external factors (e.g. by agonists, shear stress, collisions, which we do not model explicitly), and are now secreting. If m' of these secreting platelets are immediately next to a naive platelet (within the distance over which the stimulant level,  $c_0$ , secreted by a platelet is maintained), they generate a maximal agonist concentration  $c' = m' \, c_0$  in their immediate vicinity, where the naive platelet resides. To activate a naive platelet with threshold concentration c, it requires that c' > c, and thus,

$$m = \left\lceil \frac{c}{c_0} \right\rceil \tag{1}$$

is the minimal number of secreting platelets required to activate that platelet (see illustration in Fig. 1). Hence, we can formally write the events of this model as:

$$N_m + mA_s \rightarrow (m+1)A_s, \quad A_s \rightarrow A_i$$
 (2)

The first term describes how m activated secreting platelets,  $A_s$ , turn a naive platelet,  $N_m$ , into another activated secreting platelet. The second term denotes that a secreting activated platelet stops secreting after some time and becomes an idle activated platelet  $A_i$ . Note that in principle also higher numbers of co-located secreting platelets m'>m can activate a platelet, but the probability for this to happen decreases exponentially with m', and can thus be neglected.

As the population is well mixed, we can use the law of mass action to derive a dynamical model for the concentrations of naive platelets,  $n_m$ , secreting activated platelets,  $a_s$ , and idle activated platelets,  $a_i$ , from the "reactions" (2):

$$\dot{n}_{m} = -\omega n_{m} a_{s}^{m} 
\dot{a}_{s} = \omega n_{m} a_{s}^{m} - \gamma a_{s} 
\dot{a}_{i} = \gamma a_{s} ,$$
(3)

where  $\dot{x}:=\frac{dx(t)}{dt}$  for  $x=n_m,a_s,a_i$ , while  $\omega$  is the specific activation rate. This rate depends on the range a secreting platelet travels during the time it keeps secreting ("degranulation time"  $t_s$  (Polasek, 2006)), the signalling range, and the propensity to activate  $\tilde{\omega}$  (as in Fig. 1). The parameter  $\gamma=\frac{1}{t_s}$  is the rate at which a previously activated platelet ceases secreting stimulants.

Notably, for m=1, this model is equivalent to the SIR model, the paradigmatic model for the spread of a contagion (Kermack and McKendrick, 1927). In the context of infectious diseases, the case m>1 can be seen as a variant of the SIR model in which several infected individuals need to be present at the same time to infect others, i.e. they "cooperate" to spread the contagion. We therefore refer to this model, in its general form, as a *cooperative SIR model*. The following analysis will study this model, and its heterogeneous version, for its general properties.

To simplify the analysis, we will use a non-dimensionalised version of Eqs. (3), in which we use the degranulation time as time unit. Thus, we use rescaled time  $\tilde{t}=\gamma t$ , and the reproductive number  $r=\frac{\omega\rho}{\gamma}$ , where  $\rho=n+a_s+a_i$  is the total concentration of platelets. Furthermore, we express the equations in terms of the proportions of subpopulations,  $\tilde{n}=\frac{n}{\rho}, \tilde{a}_s=\frac{a_s}{\rho}, \tilde{a}_i=\frac{a_i}{\rho},$  so that  $\tilde{n}+\tilde{a}_s+\tilde{a}_i=1$ . We can then eliminate  $\tilde{a}_i=1-\tilde{n}_m-\tilde{a}_s$ , and express the system by two equations. For convenience, we rename the non-dimensionalised quantities to remove the tilde:  $\tilde{n}_m\to n_m, \tilde{a}_s\to a_s, \tilde{t}\to t$ , to arrive at the non-dimensional form of Eq. (3):

$$\dot{n}_m = -rn_m a_s^m \tag{4}$$

$$\dot{a}_{\scriptscriptstyle S} = r n_{\scriptscriptstyle m} a_{\scriptscriptstyle S}^{\scriptscriptstyle m} - a_{\scriptscriptstyle S} \ . \tag{5}$$

#### 2.3. Model for heterogeneous platelet population

We will also study a heterogeneous version of the model. First, we note that heterogeneity in r is not qualitatively different to a homogeneous system. Assuming a distribution of naive platelets with different r, n(r), we have, instead of Eq. (5),  $\dot{a}_s = \int_0^\infty r \, n(r) a_s^m \, dr - a_s$ . Since  $a_s^m \int_0^\infty r \, n(r) dr = \bar{r} n a_s$ , where  $\bar{r}$  is the mean value of r, the corresponding equation is the same as (5) when replacing r with  $\bar{r}$ . Thus, we do not consider this type of heterogeneity explicitly. Another type of heterogeneity is when the threshold concentration c varies between platelets, according to a probability density distribution n(c). Associated with this are sub-populations  $n_m$  with different threshold numbers m=1,2,..., which are related to n(c) by  $n_m=\int_{mc_0}^{(m+1)c_0} n(c) \, dc$ . Then, we get the non-dimensionalised time evolution of the system:

$$\dot{n}_m = -rn_m a_s^m \quad \text{for all } m \in \mathbb{N}$$
 (6)

$$\dot{a}_s = r \sum n_m a_s^m - a_s \ .$$

While the sensitivity of a platelet is not relevant for the dynamics after it is activated, we will for our analysis also distinguish activated platelets by sensitivity, defining the proportions of activated platelets with activation threshold m as  $a_m := a_s^{(m)} + a_i^{(m)} := n_m(t=0) - n_m$  for m=1,2,..., when using the initial condition that at time  $t=0, a_s=0$ .

#### 3. Results

#### 3.1. Collective activation

Our main goal of this section is to assess under which circumstances a macroscopic population of activated platelets,  $a:=a_s+a_i=1-\sum_m n_m$ , emerges, if initially only a microscopic (i.e. infinitesimal) population of the size  $a_s=\epsilon\to 0$  of secreting activated platelets is present, if external stimulant is absent or only microscopic. For a convenient terminology, we define the terms "microscopic"/"macroscopic", as follows: We consider a total of X platelets (or, alternatively, stimulant molecules), which is large, that is,  $X\to\infty$ , and a sub-population thereof with  $X_s$  platelets. The sub-population  $X_s$  is microscopic, if  $X_s>0$ , but its proportion on the total population  $X_s$ ,  $X_s:=\lim_{X\to\infty}\frac{X_s}{X}=0$ . On the other hand, a population is macroscopic if  $X_s$  diverges for  $X\to\infty$ , in a way that the proportion  $X_s$  is non-zero,  $X_s$  in a

#### 3.1.1. Macroscopic activation of hyper-sensitive platelets (m = 1)

The question, under which circumstances a macroscopic population of activated platelets a emerges from an initially microscopic one  $(a_s(t=0)=\varepsilon\to 0)$ , is equivalent to asking under which circumstances an epidemic breaks out in a contagion model such as the SIR model. Since for m=1, the model (4),(5) is equivalent to the SIR model, it is well known that the condition for an epidemic to break out is for r>1, if initially all individuals, except for a microscopic proportion, are susceptible — which in our case corresponds to all but a few platelets being naive.

We now wish to study this question for general m > 1 in Eqs. (4),(5) and then for the heterogeneous model, Eq. (6). We first note that the condition for a macroscopic platelet population to become activated upon exposure to a microscopic population of secreting activated platelets,  $a_s(t=0) = \epsilon \to 0$ , is equivalent to the fixed point  $x^* = (n=1, a_s=0)$  being unstable (Strogatz, 1994). Thus, to assess this, we have a look at the Jacobian matrix of Eqs. (4),(5) at that fixed point for m > 1,

$$J|_{x^*} = \begin{pmatrix} -ra_s^m & -rmna_s^{m-1} \\ ra_s^m & rmna_s^{m-1} - 1 \end{pmatrix}|_{(n=1,a_s=0)} = \begin{pmatrix} 0 & 0 \\ 0 & -1 \end{pmatrix} . \tag{7}$$

This matrix has eigenvalues 0 and -1, therefore the fixed point is Lyapunov stable (Strogatz, 1994), and not unstable for any value of r. This means that for m>1, no macroscopic activation of the platelet population can occur when seeded with an infinitesimally small population of activated platelets,  $a_s(t=0)=\epsilon$ . This has some advantages from the biological point of view: since macroscopic activation of platelets can lead to blood clotting, and inadvertent clotting can lead to dangerous pathologies through thrombosis, it could be a dangerous situation if a tiny population of such platelets were sufficient to trigger this. Hence, a situation with m>1 is protecting against inadvertent clotting.

However, it has been shown that platelet sensitivity is highly heterogeneous (Jongen et al., 2020), therefore, we study under which circumstances the heterogeneous model, Eq. (6), with a distribution of platelet thresholds  $n_m(t=0)=n_m^{(0)},\ m=1,2,...$ , can lead to macroscopic activation. Taking the Jacobian matrix of the heterogeneous model, Eq. (6), gives:

$$J = \begin{pmatrix} -ra_s & 0 & 0 & \cdots & -rn_1 \\ 0 & -ra_s^2 & 0 & \cdots & -2rn_2a_s \\ \vdots & \vdots & \cdots & \vdots & \vdots \\ ra_s & ra_s^2 & \cdots & \cdots & r\sum_m mn_m a_s^{m-1} - 1 \end{pmatrix},$$
(8)

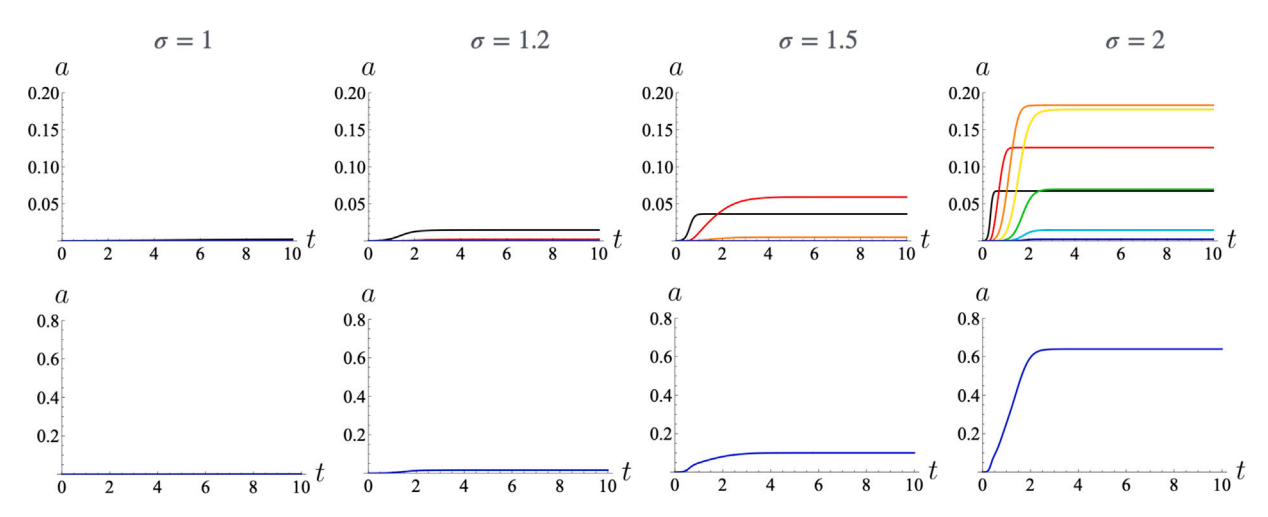


**Fig. 2.** Time course of proportion of activated platelets,  $a = a_e + a_i$  as predicted from model (6) for r = 300 and initial platelet sensitivities,  $n_m^{(0)}$ , being distributed normally with mean  $\bar{m} = 4$  and different values of standard deviation  $\sigma$  (see text for normalisation of distribution to discrete values). We have, from left to right,  $\sigma = 1, 1.2, 1.5, 2$ . The initial conditions are  $n_m(t = 0) = n_m^{(0)}$ ,  $a_s(t = 0) = 0.0001$ . (Top row:) Activated platelets separated for their initial sensitivities,  $a_m = n_m^{(0)} - n_m$ , with m = 1 (black), m = 2 (red), m = 3 (orange), m = 4 (yellow), m = 5 (green), m = 6 (cyan), m = 7 (blue). (Bottom row:) Total proportion of activated platelets  $a = a_e + a_i$ 

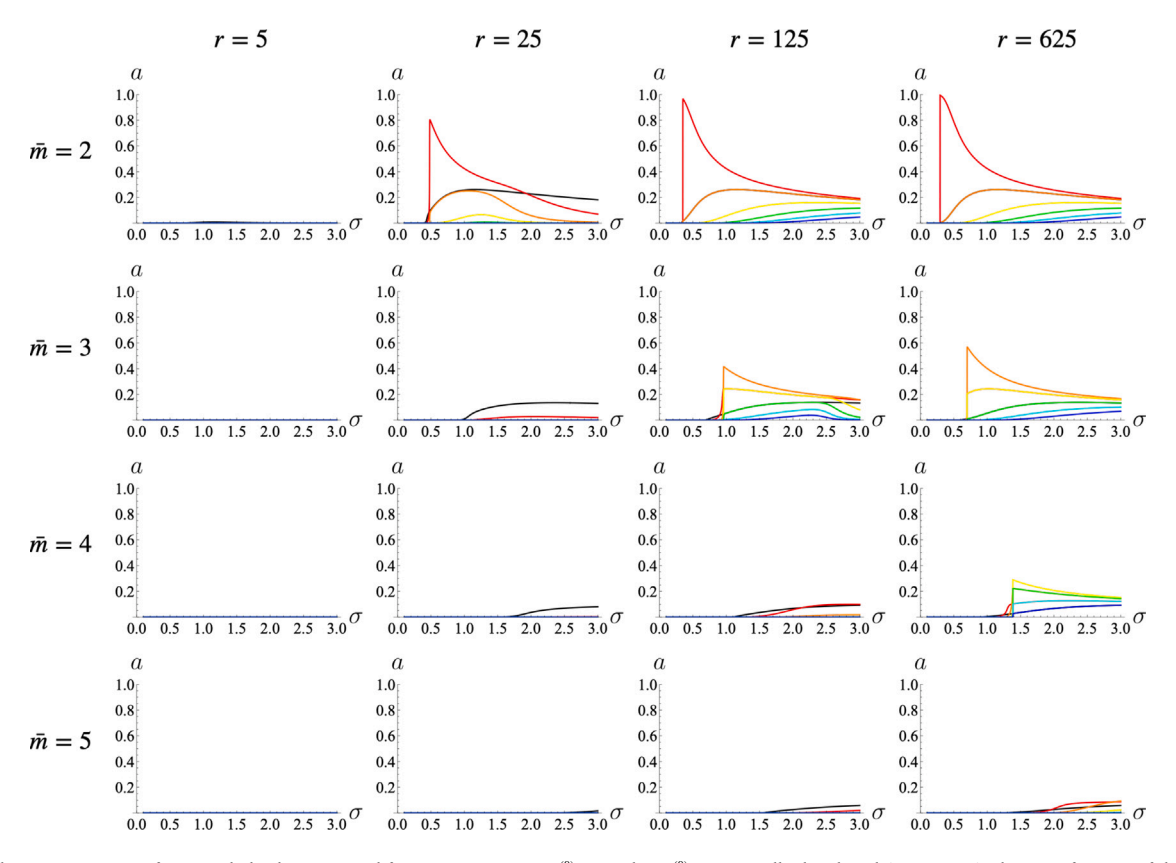


**Fig. 3.** Equilibrium proportions of activated platelets separated for sensitivities,  $a_m = n_m^{(0)} - n_m$ , when  $n_m^{(0)}$  are normally distributed (as in Fig. 2), shown as function of the width of the sensitivity distribution,  $\sigma$ , for time t = 10, as predicted by model (6). Plots are shown for different values of the distribution's mean  $\bar{m}$  (rows) and r (columns). Rows have, from top to bottom,  $\bar{m} = 2, 3, 4, 5$ , columns have, from left to right, r = 5, 25, 125, 625. Colours represent  $a_m$  for different m as in Fig. 2. The initial conditions are  $n_m(t = 0) = n_m^{(0)}, a_s(t = 0) = 0.0001$ .

where the size of the matrix is  $m_{\max} + 1$  with  $m_{\max}$  being the largest m for which  $n_m^{(0)} > 0$ . Taking the Jacobian at the fixed point  $n_m = n_m^{(0)}$  for  $m = 1, 2, \ldots$  and  $a_s^{(0)} = 0$ , we get,

$$J = \begin{pmatrix} 0 & 0 & 0 & \cdots & -rn_1^{(0)} \\ 0 & 0 & 0 & \cdots & 0 \\ \vdots & \vdots & \cdots & \vdots & \vdots \\ 0 & 0 & \cdots & \cdots & rn_1^{(0)} - 1 \end{pmatrix} . \tag{9}$$

This is a triangular matrix, which thus has the eigenvalues 0 (with multiplicity  $m_{\rm max}$ ) and  $r\,n_1^{(0)}-1$ . As the latter eigenvalue is positive

for  $rn_1^{(0)}>1$ , we get that for those values the fixed point is unstable and thus a macroscopic proportion of the platelet population becomes activated, while for  $rn_1^{(0)}<1$ , no macroscopic activation occurs, i.e.  $a\approx 0$ . For notational convenience, we thus call  $n_1^*:=\frac{1}{r}$  and  $r^*:=\frac{1}{n_1^{(0)}}$ , respectively, the critical values which, when exceeded, lead to macroscopic activation. This is not surprising, since the sub-population of hyper-sensitive platelets, with m=1, follows the dynamics of the SIR model. In that case (when  $rn_1^{(0)}>1$ ), we have that  $\dot{a}_s>rn_1-1>0$  as long as  $n_1>\frac{1}{r}$ . Since the activation wave ceases only once  $\dot{a}\leq 0$ , this

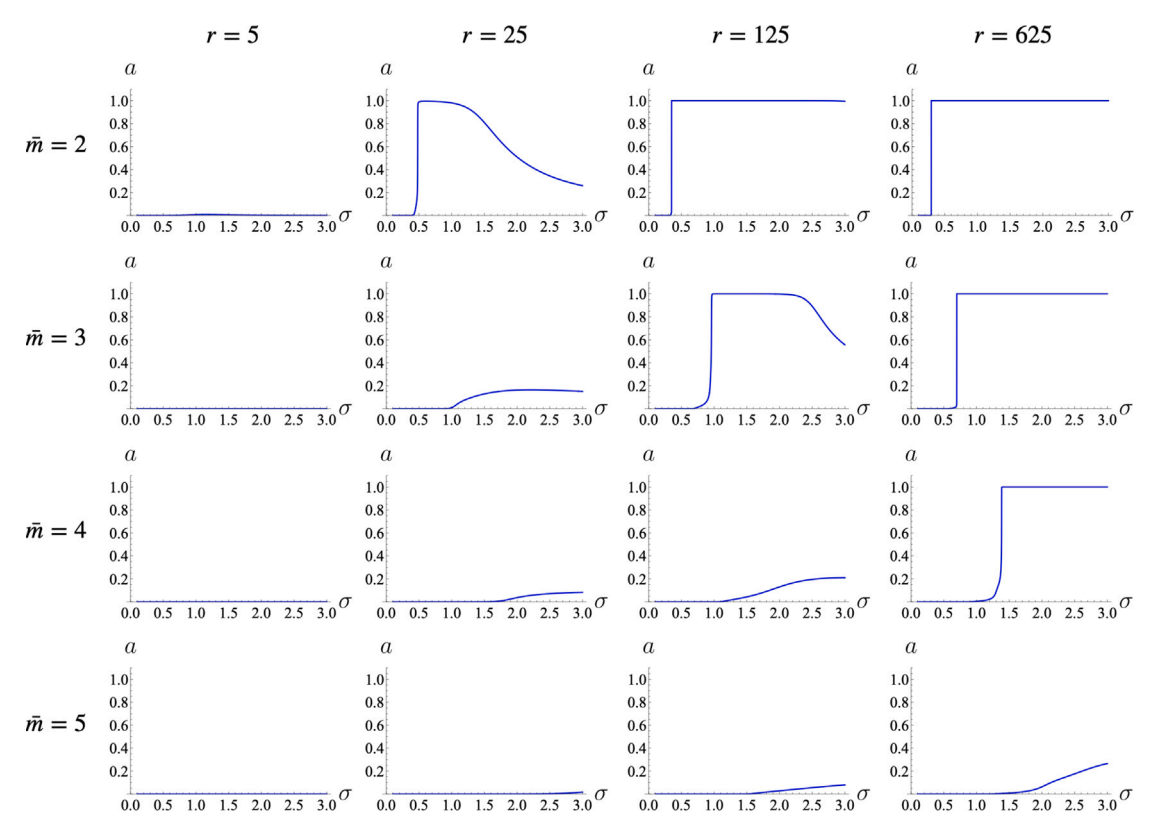


Fig. 4. Equilibrium values of the total proportion of activated platelets,  $a = a_e + a_t$ , when  $n_m^{(0)}$  are normally distributed (as in Fig. 2), as function of the width of the sensitivity distribution,  $\sigma$  (see Fig. 2), for non-dimensionalised time t = 10, as predicted by model (6). Plots are shown for different values of the distribution's mean  $\bar{m}$  (rows) and signalling parameter r (columns). Rows have, from top to bottom,  $\bar{m} = 2, 3, 4, 5$ , columns have, from left to right, r = 5, 25, 125, 625. The initial conditions are  $n_m(t = 0) = n_m^{(0)}, a_v(t = 0) = 0.0001$ .

means that eventually  $n_1 < \frac{1}{r}$ , and thus the final proportion of activated platelets, for  $t = t_f \to \infty$ , has a lower bound:  $a = n_1^{(0)} - n_1 > n_1^{(0)} - \frac{1}{r}$ .

## 3.1.2. Macroscopic activation of less sensitive platelets (m > 1)

At first glance, it is only obvious that the sub-population of platelets with m = 1 is activated, while it is not clear whether platelets with less sensitivity, that is, higher thresholds of m, will be activated to macroscopic proportions. To assess this, we consider numerical solutions of Eqs. (6), restricted to  $m = 1, ..., m_{\text{max}}$  with  $m_{\text{max}} = 12$ , to ensure a finite number of equations. We solved these for different distributions of platelet sensitivities and values of r. We first consider the scenario where platelet sensitivities are distributed according to a Normal distribution  $\mathcal{N}_{\bar{m},\sigma}$  with mean activation threshold  $\bar{m}$  and standard deviation  $\sigma$ . Here, we adapt the Normal distribution to return probabilities only at discrete values  $m=1,\ldots,m_{\max},$  by normalising it so that  $\sum_{m=1}^{m_{\max}} \mathcal{N}_{\bar{m},\sigma}(m) = 1$ . In Fig. 2 we see time courses of activation, separated for platelets with different m, with  $a_m = n_m^{(0)} - n_m$  for fixed  $\bar{m} = 4$  and different values of  $\sigma$ . Notably, we see that for low values of  $\sigma$ , no macroscopic activation occurs, for larger values, activation occurs, but only for population  $n_1$ , while for even larger values activation of populations  $n_m$  with higher m > 1 occurs as well. Thus, we observe that in a heterogeneous population, the population with the highest sensitivity m = 1, but also populations with the lower sensitivity (larger m > 1) are activated if signalling strength r and heterogeneity, characterised by  $\sigma$ , are sufficiently high.

To further assess how the mean sensitivity and the heterogeneity of the sensitivity affect the collective activation of platelets, we show in Figs. 3 and 4 the end points of the time courses of Fig. 2 (as the curves reach a plateau) as a function of the standard deviation of the sensitivity distribution,  $\sigma$ . Total activated proportions a (Fig. 4) and individual proportions  $a_m$  (Fig. 3, as curves of different colours) are shown for various values of  $\bar{m}$  and r. We see that for fixed values

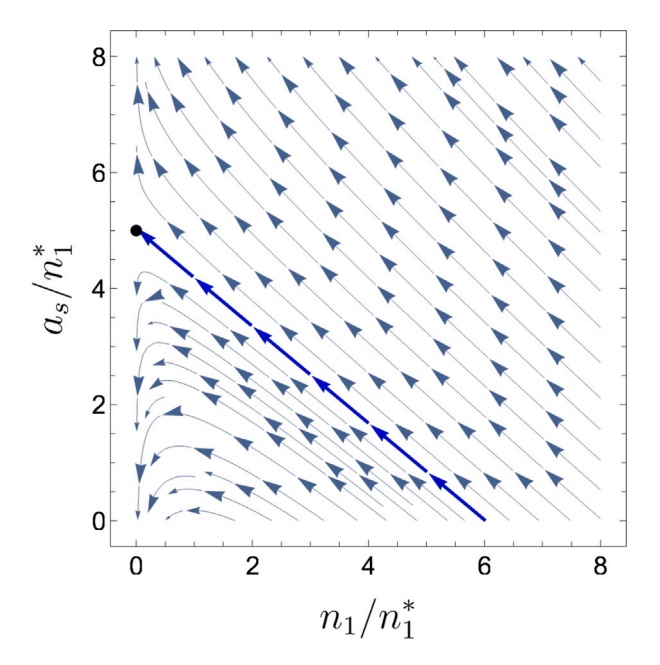


**Fig. 5.** Phase portrait projected on  $a_s, n_1$  (collection of trajectories  $a_s(n_1)$ ), rescaled by  $n_1^* = \frac{1}{r}$  for small  $a_s$  when  $O(a_s^3)$  can be neglected and  $n_m \approx const$  for m > 1. Parameter r = 100. The emphasised blue trajectory shows the trajectory converging to the fixed point  $(n_1 = 0, a_s = \frac{1}{n_2})$ , given by Eq. (11). This trajectory denotes the stable manifold which separates basins of attraction.

of  $\bar{m}$ , but small heterogeneity  $\sigma$ , there is no macroscopic activation, but as the heterogeneity increases, macrosopic activation with a>0 occurs. For small values of r, we see that when increasing  $\sigma$ , first only the population with m=1 is activated and then, for higher  $\sigma$ 

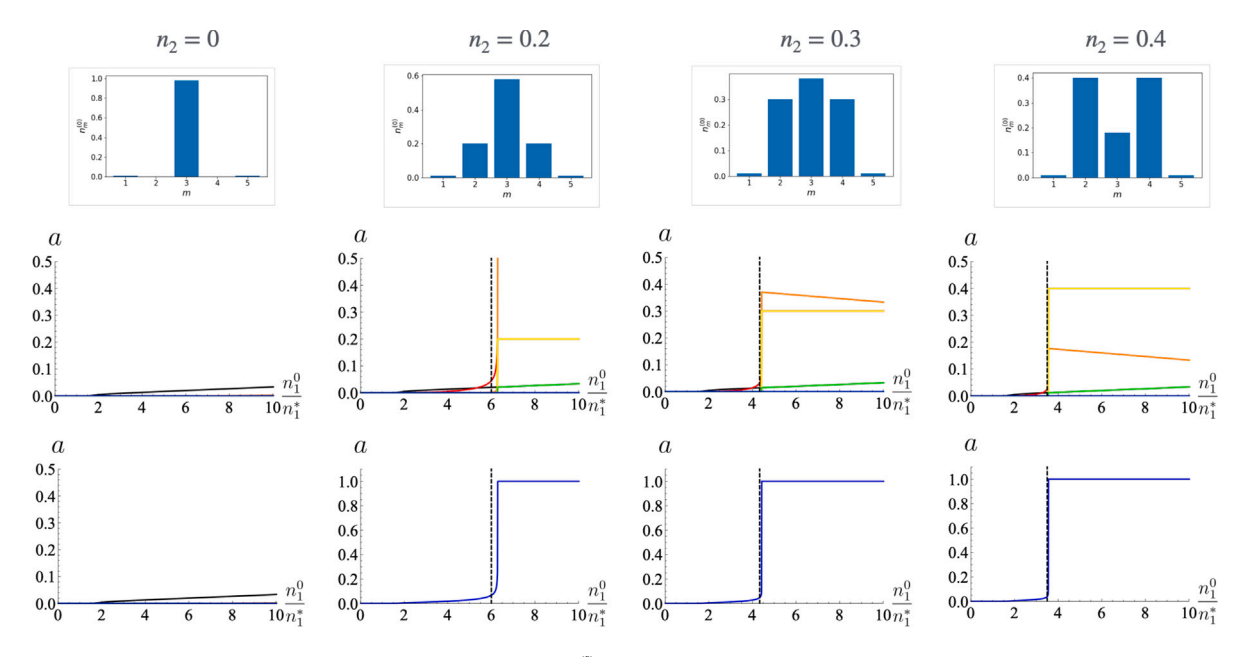


**Fig. 6.** Equilibrium proportions of activated platelets,  $a=a_s+a_i$ , as function of  $n_1^{(0)}$ , rescaled by  $n_1^*=1/r$ . The plots show different values of  $n_2$  in different columns, from left to right  $n_2=0,0.2,0.3,0.4$ . We assume a symmetric distribution with  $\bar{m}=3$ , which further implies  $n_3^{(0)}=1-2n_1^{(0)}-2n_2^{(0)},n_4^{(0)}=n_2^{(0)},n_5^{(0)}=n_1^{(0)}$ . The vertical dashed line indicates the critical value  $n_1^{**}=n_1^*+\frac{1+n_2}{n_2}$ . The initial conditions are  $n_m(t=0)=n_m^{(0)},a_s(t=0)=10^{-6}$  (Top row:) Illustration of the distributions  $n_m^{(0)}$  for  $m=1,2,\ldots,5$  used below. (Middle row:) activated proportions separated by  $m_1$ ,  $m_2$ ,  $m_3$ ,  $m_4$ ,  $m_2$ ,  $m_3$ , (Bottom row:) Total activated proportion  $m_1$ .

populations with lower sensitivity (m>1) are activated. Notably, for higher r, the activated proportions of the populations with m>1 exceed substantially the activated population with m=1. Since we know that lower sensitive populations with m>1 cannot be activated macroscopically by microscopic  $a_s$ , it appears that the population with m=1 is initially activated, generating a non-zero proportion  $a_s$ , which serves as a 'seed' to activate lower sensitive populations. This activation may then sustain itself if  $a_s$  is large enough.

In order to understand this behaviour, we study analytically under which circumstances the population of activated platelets remains small, i.e. when  $a\ll 1$  and thus  $a_s\ll 1$ . We wish to study this for arbitrary distributions of platelet sensitivities  $n_m(t=0)=n_m^{(0)}, m=1,2,...$ , but focus on situations where the population of hypersensitive platelets with m=1 is very small, while the other populations are much larger:  $n_1^{(0)}\ll 1$  and  $n_m^{(0)}\gg n_1^{(0)}$  are such that  $\frac{n_1^{(0)}}{n_m^{(0)}}\sim O(a_s)\ll 1$  for all m>1. Furthermore, since macroscopic activation can only occur for  $n_1^{(0)}>\frac{1}{r}$  we additionally assume that  $n_1^*=\frac{1}{r}\ll 1$ , that is, r is large. This is also a biologically realistic regime: as the degranulation time is around 60s (Polasek, 2006), which is roughly the time blood circulates once through the entire circulatory system, any secreting platelet can potentially get in contact with a very large number of naive platelets and activate them.

Since, according to these assumptions,  $a_m \ll 1$ , we can assume  $n_m \approx n_m^{(0)}$  being approximately constant for m>1, and it is therefore sufficient to consider only  $n_1, a_s$  as dynamical variables. We note that the first two terms of Eq. (6),  $rn_1a_s$  and  $rn_2a_s^2$  are both of order  $O(a_s^2)$  while the other terms are of order  $O(a_s^3)$ , thus we have, in leading order of (small)  $a_s$  for Eq. (6):

$$\dot{n}_1 = -rn_1 a_s 
\dot{a}_s = rn_1 a_s + rn_2 a_s^2 - a_s + O(a_s^3) \approx rn_1 a_s + rn_2 a_s^2 - a_s.$$
(10)

We can now study the fixed points of this system when neglecting  $O(a_s^3)$ . We see that there are fixed points for any  $a_s=0$ , and there is one fixed point for  $a_s>0$ , namely for  $n_1=0$  and  $a_s=\frac{1}{n_2r}=:a_s^*$ . A linear stability analysis (see Appendix) shows that this is a saddle point, which means that there is a stable manifold, which, since this is a two-dimensional system, consists of the trajectories that converge

to the point  $x^* = (n_1 = 0, a_s = \frac{1}{n_2 r})$ . This stable manifold separates the phase space into two basins of attraction, one which converges to  $a_s = 0$  and one where trajectories diverge. To illustrate this, we show the phase portrait of system (10) for r = 100 in Fig. 5. Here, we see that the highlighted trajectory separates the other trajectories according to their fate. If  $n_1^{(0)}$  lies below this curve,  $a_s$  cannot exceed  $a_s^* = \frac{1}{n_2 r}$ . On the other hand, if it lies above that curve,  $a_s$  will diverge, meaning that our approximation will break down and thus  $a_s \gg \frac{1}{n_2 r}$ .

To find the stable manifold which separates basins of attraction, we express trajectories as functions  $a_s(n_1)$  in the  $n_1$ - $a_s$ -plane. They can be found as solutions to the differential equation,

$$\frac{da_s}{dn_1} = \frac{\frac{da_s}{dt}}{\frac{dn_1}{dt}} \approx -1 - \frac{n_2}{n_1} a_s(n_1) + \frac{1}{rn_1} \ . \tag{11}$$

This is a linear ordinary differential equation, whose solution can be found, for example, by the integrating factor method. As we are looking for a trajectory converging to  $(n_1 = 0, a_s = \frac{1}{n_2 r})$ , we can choose the initial condition  $a_s(n_1 = 0) = \frac{1}{n_2 r}$ , and with this we get the solution,

initial condition 
$$a_s(n_1=0)=\frac{1}{n_2r}$$
, and with this we get the solution, 
$$a_s(n_1)=\frac{1+n_2-rn_1n_2}{rn_2(1+n_2)} \ . \tag{12}$$

Furthermore, since  $\dot{n}_1 < 0$ , the direction of this trajectory is towards  $x^*$ , hence this is indeed the stable manifold. Now, we need to distinguish whether  $n_1^{(0)}$  is below or above that trajectory. To this end, we determine the intersection of this trajectory with the  $n_1$  axis, which we find as the solution to  $0 = \frac{1+n_2-rn_1n_2}{rn_2(1+n_2)}$ , which is  $n_1^{**} = \frac{1+n_2}{rn_2}$ . Hence, for  $n_1^{(0)} < n_1^{**}$ ,  $a_s$ , and thus a, remain below  $a_s^* = \frac{1}{n_2r}$ , while for  $n_1^{(0)} > n_1^{**}$ ,  $a_s$ , and thus a, exceed this value substantially. Note that in the case  $r \to \infty$ ,  $\frac{1}{n_2r} = a_s^*$  must be microscopic, so the condition for a remaining microscopic is  $n_1^{(0)} < \frac{1+n_2}{rn_2}$ . In that case, we thus get that substantial proportions of  $a_m$  emerge once  $n_1^{(0)}$  exceeds  $n_1^{**} = n_1^* \frac{1+n_2}{n_2}$ . This is shown in Fig. 6 to be an accurate prediction: there, final activation a is shown as function of  $n_1$  for different values of  $n_2$  and a mean value  $\bar{m} = 3$ , and the dashed line shows the predicted value  $n^{**}$  for the transition towards macroscopic activation.

This demonstrates that a microscopic proportion of hyper-sensitive platelets,  $n_1^{(0)}$ , is sufficient to trigger a macroscopic activation also

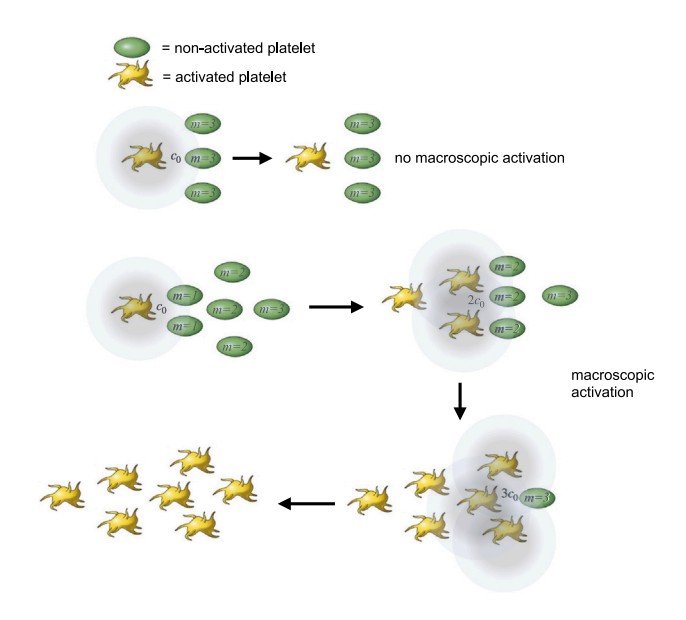


**Fig. 7.** Illustration of the mechanism driving macroscopic activation in heterogeneous platelet populations. Black arrows denote changes in the population over time, grey areas denote activation signal ranges. (Top:) platelets with lower sensitivity (here m=3) cannot be activated by a single platelet. (Middle/bottom:) If hyper-sensitive platelets with m=1 and higher-than-average sensitivity (here: m=2) are present, a cascade of intermediate activation, first of the m=1 population and then of the m=2 population, allows also the activation of the less sensitive m=3 population.

of platelet populations with less sensitivity, m>1, including those with average sensitivity  $\bar{m}$ . Nonetheless, for  $n_2^{(0)}=0$ , no substantial activation is observed. Thus, we conclude that the presence of platelets with intermediate sensitivity, between hyper-sensitivity with m=1, and mean sensitivity  $\bar{m}$ , are essential for macroscopic activation (see ilustration in Fig. 7). Although we do not have analytical means to study further terms in Eq. (6), we expect that more populations with m>2 can further amplify the spread of the activation signal if  $n_m^{(0)}\gg n_1^{(0)}$ , as has been indicated above in Figs. 2–4.

#### 3.2. Comparison with experiments with external stimulants

We now consider the situation where an external stimulant (agonist) is present which is able to directly activate platelets. We assume that the stimulation of this agonist and that of signalling molecules emitted by secretory platelets add up, so that the total stimulant concentration in the vicinity of m platelets is  $c' = c_{ex} + mc_0$ , where  $c_{ex}$  is an concentration equivalent of externally provided stimulant. Hence, the threshold number of secreting platelets m required to activate platelets with threshold concentration c is  $m = \lceil \frac{c - c_{\text{ex}}}{c} \rceil$ . Therefore, given a probability density distribution n(c) of platelets with threshold concentrations c, we get a distribution of initially naive platelets of  $n_m = n_{\lceil \frac{c+c_{\mathrm{ex}}}{\rceil} \rceil}$ . This means that with increasing  $c_{\mathrm{ex}}$ , the distribution  $n_m$ gets shifted towards lower m. Importantly, platelets with  $c < c_{ex}$  are activated from the beginning, when the stimulant is given. We thus have as initial condition  $a_s(t=0) = \int_{c < c_{\rm ex}} n(c) dc \approx \sum_{m < \frac{c_{\rm ex}}{c_{\rm p}}} n_m$ . Hence, with increasing  $c_{\rm ex}$ , both the proportion of initially secreting activated platelets increases, and the distribution of platelets is shifted towards lower m, consequently enhancing activation.

We wish to compare our model predictions with experimental results from droplet microfluidics assays with platelets, performed by Jongen et al. (2020). In one of those experiments, platelets were enclosed in micro-droplets and exposed to the external stimulant convulxin, at varying concentration, and then the abundance of the activation marker P-selectin was measured via fluorescent cytometry, that is, the fluorescent intensity, I, was recorded (Fig. 2B in Jongen et al.

(2020)). Two scenarios are compared: (A) where each droplet contains a single platelet, (B) where droplets contain platelet collectives. In situation (A) no platelet can activate another platelet through paracrine signalling since they are separated by droplets, hence  $c'=c_{\rm ex}$  and thus the proportion of activated platelets at a given concentration  $c_{\rm ex}$  of convulxin is the cumulative distribution  $F(c_{\rm ex})=a_s(t=0)=\int_{c< c_{\rm ex}} n(c) dc$ . Hence, the distribution of sensitivities can directly be inferred from this data. In scenario (B), platelets can activate each other, and thus this measures the collective activation of a platelet population. This can be compared with the predicted proportion of activated platelets, a, from our model.

However, our model has limitations modelling this data, as the experimental setup does not meet all assumptions of our model. In particular, since platelet collectives are encapsulated in a flow-free confined environment (droplets), the agonists secreted by platelets are not quickly dispersed, and thus can accumulate and reach platelets which are even further away. This means that we can expect an enhanced paracrine activation between platelets, resulting in a higher value of r than would be expected in an in vivo situation. Nonetheless, we wish to test whether the *qualitative* behaviour, namely the predicted collective activation of the population through a small, hyper-sensitive population of platelets, prevails. To that end, rather than finding accurate precise numerical model fits, we explore the parameter space to find values for which the model qualitatively reproduces the data.

To determine an estimate for the distribution n(c) and thus  $n_m$ , we fit a cumulative distribution function to the data of single-platelet droplets (A). First, we need to renormalise the experimental fluorescence measurements, I, from Jongen et al. (2020), as there is some background P-selectin expression even in absence of activation. Hence, we define the *relative activation* as  $a_{\rm exp}=\frac{I-I_{\rm min}}{I_{\rm max}-I_{\rm min}}$  where  $I_{\rm min}$  and  $I_{\rm max}$  are minimum and maximum fluorescence values. As the data in Jongen et al. (2020) shows a symmetric sigmoidal form on a logarithmic scale of c, we will attempt to fit a log-normal distribution, with mean  $\bar{c}$  and logarithmic variance  $\sigma_c^2$  to the data. For an easier comparison with our model, which uses  $m=\frac{c}{c_0}$  to define platelet populations, we will try only values  $\bar{c}=\bar{m}c_0$  and  $\sigma_c=\sigma_mc_0$  with integer  $\bar{m},\sigma_m=1,2,...$  To that end, we first need to find an estimate for  $c_0$ . As for  $c_{\rm ex}=c_0$  the sub-population with m = 1 is being activated for the first time upon increasing values of  $c_{\rm ex}$ , we identify  $c_0$  as the concentration for which, upon increasing concentrations of  $c_{\rm ex}$ , for the first time substantial collective activation emerges in data (B). While due to the lack of intermediate data points, this estimate can only be a rough one, we can estimate this from inspection of data (B) to be around  $c_0 = 0.3$ ng/mL. While some activation is present already at  $c_{\rm ex} = 0.1$  ng/mL, this could be due to spontaneous activation that is expected from our model according to our previous discussion.

We find that for  $\bar{m}=14$  and  $\sigma_m=2$ , corresponding to  $\bar{c}=4.2$  ng/mL and  $\sigma_m=0.6$  ng/mL, a good match of the log-normal distribution with the single-platelet droplet data, (A), is achieved, as is shown in Fig. 8A. We will thus use  $n_m^{(0)}=\mathcal{N}e^{-\frac{(\ln m-\ln \bar{m})^2}{2\sigma_m^2}}$  as the initial distribution of platelet

We will thus use  $n_m^{(0)} = \mathcal{N}e^{-2\sigma_m^2}$  as the initial distribution of platelet activation thresholds in absence of external stimulant, where  $\mathcal{N}$  is a normalisation factor that accounts for the discreteness of the values m (in the same way as was done in the previous section). Then, we determine the initial distribution of platelet sensitivities with external stimulant  $c_{\rm ex}$  as  $n_m(t=0)=n_{\lfloor m+c_{\rm ex}/c_0\rfloor}^{(0)}$  and  $a_s(t=0)=\sum_{m<\frac{c_{\rm ex}}{c_{\rm ex}}}n_m^{(0)}$ , and we solve the system (6) numerically using Scipy's solve\_ivp function. The end points (at time t=10) of those solutions are shown in Fig. 8B for different values of r, together with the experimental data of platelet collectives in droplets from from Jongen et al. (2020). We note that for smaller values of r no reasonable match is achieved, but for very high values of r, in particular for  $r=30\,000$  (green curve in Fig. 8B), a good qualitative agreement is achieved. This is consistent with the expectation that due to the accumulation of paracrine signalling molecules within droplets, a single platelet can reach and activate a much higher population of platelets than would be in an

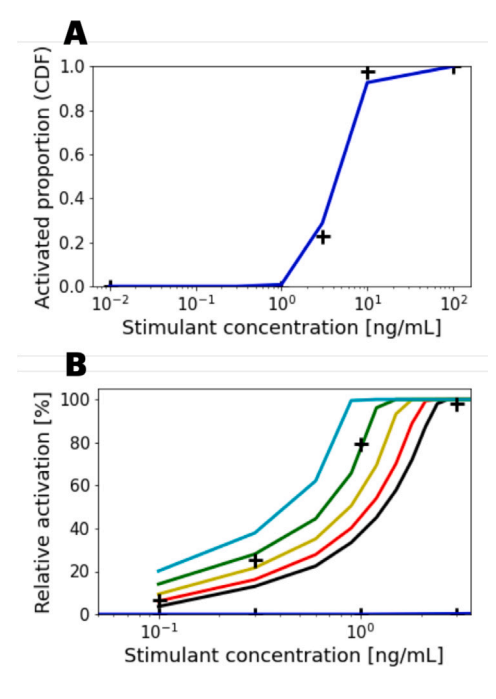


**Fig. 8.** Comparison with experimental results from Jongen et al. (2020). Pluses show experimental results measuring overall P-selectin activity (a marker for platelet activation) as fluorescence levels via flow cytometry, rescaled for background fluorescence and as proportion of maximal fluorescence (see text). Error bars are smaller than the symbol sizes. Curves show model predictions for  $a = a_e + a_i$ . The horizontal axis shows varying concentrations of stimulant (convulxin) to which platelets were exposed in the experiments, the *y*-axis shows relative activation. (A) Shows a log-normal distribution with mean c = 4.2 ng/mL and standard deviation σ = 0.6 ng/mL, together with experimental results from Jongen et al. (2020) where single platelets are encapsulated in single droplets. This is a proxy for the cumulative probability distribution (*CDF*)  $F(c) = \int_{c'<c} n(c') dc'$ . (B) Shows model output for a, compared with experimental results from Jongen et al. (2020) with platelet collectives in single droplets, for different values of r: r = 1000 (black), r = 3000 (red), r = 10000 (orange), r = 30000 (green), r = 100000 (cyan).

*in vivo* flow environment. Overall, this demonstrates that our model is able to qualitatively reproduce the experimental data on collective platelet activation, though at parameter values which are likely beyond the corresponding *in vivo* values.

#### 4. Discussion

Blood clotting is an important physiological process, but when it occurs inadvertently, it can cause thrombosis which can be live threatening. Thus, understanding and eventually predicting blood clotting can aid in preventing thrombosis. The initiating stage on the path towards blood clotting is the collective activation of platelets, hence understanding the platelet activation dynamics will aid in assessing blood clotting risk.

We have introduced a minimal model for the activation dynamics of blood platelets via paracrine, platelet-platelet signalling. In particular, we considered the scenario when platelets are immersed in blood flow, where due to fast dispersion of stimulants, one or more activated platelets that secret activation signals are required in the immediate vicinity of a non-activated, naive platelet, to activate the latter. From these and other biologically motivated assumptions, we formulated a minimal dynamical model, (3), for the time evolution of naive and activated platelets, with the aim to predict the proportion of activated platelets when starting with a predominantly naive platelet population, that is, with only a small number of initially activated plateles. If the number of secreting activated platelets required to activate a naive one, m, is equal to one, this model is equivalent to the SIR model – the paradigmatic contagion model – and macroscopic activation occurs

whenever the 'reproductive number' r is above a critical value, even for microscopic proportions of initially activated secreting platelets. For m>1 the model, which we then call *cooperative SIR model*, still has the characteristic of a contagion model, yet, if the population is uniform, no macroscopic activation is possible, if initially only few platelets are secreting. The formal similarity to the SIR model provides some intuitive understanding, by viewing the activation signal as a type of contagion which may or may not spread across the whole platelet population (like an 'epidemic'), depending on the circumstances.

Nonetheless, it is known that platelet sensitivity varies considerably between platelets, therefore we considered a heterogeneous version of the model, where sensitivity to activation, characterised by m, may differ between platelets. We showed that in this case, a macroscopic activation of the population is possible when only few activated platelets are initially present, if r is sufficiently high. In that case, the hyper-sensitive sub-population with m = 1 becomes activated, and this activated, secreting sub-population then serves as a 'seed' to activate sub-populations with higher m, in a staggered cascade of activating ever less sensitive sub-populations (with higher m > 1). Notably, we showed analytically and numerically that a microscopic proportion of platelets with m = 1 is sufficient to achieve this, if r is sufficiently large. This supports the hypothesis that a rare population of hyper-sensitive platelets could be able to mediate macroscopic activation and thus trigger blood clotting (Baaten et al., 2017; Jongen et al., 2020; Lesyk and Jurasz, 2019). We further showed that in order to activate the bulk of the platelet population, also platelets with less, yet higher-thanaverage sensitivity, with thresholds m between that of hyper-sensitive and average platelets (thresholds  $1 < m < \bar{m}$ ), are required (see illustration in Fig. 7). This is biologically required to then achieve macroscopic platelet aggregation and eventually blood clotting. A 'gap' in sensitivities, for example if there are no, or only few platelets with m = 2, may break the activation cascade, and no substantial activation of the platelet population as a whole emerges.

Finally, we compared our model results with experimental results where platelet activation and aggregation was measured with platelets encapsulated in micro droplets (Jongen et al., 2020). While this experimental setup did not meet all our model assumptions – in particular since secretory, stimulating signals can accumulate – we showed that our model is capable of qualitatively reproducing the observed doseresponse curves, namely the activation intensity as function of provided external stimulant, if the reproductive number  $\it r$  is very large.

Since most clinical platelet function tests measure bulk platelet properties to assess thrombosis risk (Anghel et al., 2020; Pabinger and Ay, 2009), these findings suggest that clinical practice may need to be revised: if the distribution of (higher-than average) platelet sensitivities is determining the onset of blood clotting, rather than bulk platelet sensitivity, then measurements of the former – for example via droplet microfluidics as done by Jongen et al. (2020) – would be required for an appropriate assessment of thrombosis risk.

Naturally, a simple model as the here presented one has limitations, mainly by using a well-mixed approximation, which is essential to render the model simple enough - in the form of ordinary differential equations - to allow thorough theoretical insights beyond mere numerical results. This approximation, which is widely used in population dynamics, epidemiology and chemistry, neglects the spatial structure of the population and does not consider different flow velocities between different parts of the population. For example, it does not consider the situation where activated, aggregated platelets are bound to the vessel walls and non-activated platelets being immersed in free flow, as usually occurs in physiological clotting. It does, however, consider pathological clotting when platelets within the blood flow, detached from vessel walls, activate on macroscopic scales (homogeneous flow can be accommodated by changing to the co-moving frame). The well-mixed approximation - in other fields like physics also known as "mean field approximation" - has less quantitative accuracy than more complex and spatially detailed models, yet, mean field models

as ours are known to reflect qualitative features, such as the here described transition from microscopic to macroscopic activation, and the impact of platelet diversity, rather well (Goldenfeld, 1992). The model is therefore well suited to reproduce the qualitative features of spontaneous blood clotting that is initiated away from vessel walls.

To summarise, we showed that a simple model, reminiscent of the SIR model, is able to reproduce measured qualitative features of collective platelet activation. This model explains mechanistically how, possibly very rare, hyper-sensitive platelets can serve as an activation seed for the propagation of activation through the whole population to achieve macroscopic activation, if sufficient amounts of platelets with less, but larger-than-average sensitivity are present. Once a substantial fraction of the platelet population has been activated, they may then aggregate and form the body of a blood clot. These findings may serve as a stepping stone towards the development of a comprehensive model for whole blood clotting, to allow quantitative predictions for the probability of blood clotting, and hence the risk of thrombosis.

#### Declaration of competing interest

The authors declare that they have no known competing financial interests or personal relationships that could have appeared to influence the work reported in this paper.

#### Acknowledgements

I thank Jonathan West for guidance in processing the experimental data of Jongen et al. (2020).

#### **Appendix**

We wish to analyse the stability and stable manifold of the fixed point of Eq. (10). This system has fixed points for any  $a_s = 0$  and for  $a_s = \frac{1}{r-s}$  and  $n_1 = 0$ . The Jacobian of the system at this fixed point is:

$$a_s = \frac{1}{n_2 r} \text{ and } n_1 = 0. \text{ The Jacobian of the system at this fixed point is:}$$

$$J = \begin{pmatrix} -ra_s & -rn_1 \\ ra_s & rn_1 + 2rn_2a_s - 1 \end{pmatrix} \Big|_{n_1 = 0, a_s = 1/r} = \begin{pmatrix} -\frac{1}{n_2} & 0 \\ \frac{1}{n_2} & 1 \end{pmatrix}$$
(A.1)

This matrix is in triangular form and thus has eigenvalues  $-1/n_2 < 0$  and 1 > 0. Hence it is a saddle point, which possesses a stable trajectory, which separates the space into two basins of attraction, defined as the trajectory converging to the fixed point. In the main text, we show that  $a_s(n_1) = \frac{1+n_2-rn_1n_2}{rn_2(1+n_2)}$  is this trajectory.

#### Data availability

Numerical data for Figures 2-6 was generated with Wolfram Mathematica, and for Fig. 8 with python. The Mathematica workbook and python programming code are available at <a href="https://github.com/philipgreulich/cooperative-SIR">https://github.com/philipgreulich/cooperative-SIR</a>.

### References

- Anand, M., Rajagopal, K., Rajagopal, K.R., 2003. A model incorporating some of the mechanical and biochemical factors underlying clot formation and dissolution in flowing blood. J. Theoret. Med. 5, 183–218. http://dx.doi.org/10.1080/ 10273660412331317415.
- Anghel, L., Sascău, R., Radu, R., Stătescu, C., 2020. From classical laboratory parameters to novel biomarkers for the diagnosis of venous thrombosis. Int. J. Mol. Sci. 21, http://dx.doi.org/10.3390/ijms21061920.
- Baaten, C.C., ten Cate, H., van der Meijden, P.E., Heemskerk, J.W., 2017. Platelet populations and priming in hematological diseases. Blood Rev. 31, 389–399. http: //dx.doi.org/10.1016/j.blre.2017.07.004.
- Born, G.V., 1962. Aggregation of blood platelets by adenosine diphosphate and its reversal. Nature 194, 927–929. http://dx.doi.org/10.1038/194927b0.
- British Heart Foundation, 2021. Global heart and circulatory diseases factsheet.

- Cardinal, D.C., Flower, R.J., 1980. The electronic aggregometer: A novel device for assessing platelet behavior in blood. J. Pharmacol. Meth. 3, 135–158, https://cir. nii.ac.jp/crid/1571135649084851712.
- Carubbi, E., Gesi, M., Galli, D., Mirandola, P., Vitale, M., Gobbi, G., Masselli, C., 2014. Cytofluorimetric platelet analysis. Semin. Thromb. Hemost. 40, 88–98. http://dx.doi.org/10.1055/s-0033-1363472, http://www.thieme-connect.de/products/ejournals/abstract/10.1055/s-0033-1363472.
- Donahue, S.M., Otto, C.M., 2005. Thromboelastography: A tool for measuring hyper-coagulability, hypocoagulability, and fibrinolysis. J. Veterin. Emerg. Crit. Care 15, 9–16. http://dx.doi.org/10.1111/j.1476-4431.2005.04025.x.
- Fogelson, A.L., 1993. Continuum models of platelet aggregation: Mechanical properties and chemically-induced phasen transition. Contemp. Math. 141 (279).
- Fogelson, A.L., 2016. Continuum models of platelet aggregation: Formulation and mechanical properties. SIAM J. Appl. Math. 52, 1089–1110.
- Fogelson, A.L., Neeves, K.B., 2015. Fluid mechanics of blood clot formation. Annu. Rev. Fluid. Mech. 47, 377. http://dx.doi.org/10.1146/annurev-fluid-010814-014513. Fluid
- Gale, A.J., 2011. Current understanding of hemostasis. Toxicol. Pathol. 39, 273–280. http://dx.doi.org/10.1177/0192623310389474.
- Goldenfeld, N., 1992. Lectures on phase transitions and the renormalisation group.
   Heemskerk, J.W., West, J., 2022. Emerging technologies for understanding platelet diversity. Arterioscler. Thromb. Vasc. Biol. 42, 540–552.
- Hellmuth, R., Bruzzi, M.S., Quinlan, N.J., 2016. Analysis of shear-induced platelet aggregation and breakup. Ann. Biomed. Eng. 44, 914–928. http://dx.doi.org/10. 1007/s10439-015-1409-1.
- Jongen, M.S., MacArthur, B.D., Englyst, N.A., West, J., 2020. Single platelet variability governs population sensitivity and initiates intrinsic heterotypic responses. Commun. Biol. 3 (281), http://dx.doi.org/10.1038/s42003-020-1002-5.
- Kermack, W.O., McKendrick, G.A., 1927. A contribution to the mathematical theory of epidemics. Proc. R. Soc. A 115 (700), http://dx.doi.org/10.21136/cpmf.1924. 109357.
- Koltai, K., Kesmarky, G., Feher, G., Tibold, A., Toth, K., 2017. Platelet aggregometry testing: Molecular mechanisms, techniques and clinical implications. Int. J. Mol. Sci. 18, 1–21. http://dx.doi.org/10.3390/jims18081803.
- LaPelusa, A., Dave, H.D., 2023. Physiology, hemostasis.
- Lesyk, G., Jurasz, P., 2019. Advances in platelet subpopulation research. Front. Cardiovasc. Med. 6 (138), http://dx.doi.org/10.3389/fcvm.2019.00138.
- Link, K.G., Sorrells, M.G., Danes, N.A., Neeves, K.B., Leiderman, K., Fogelson, A.L., 2020. A mathematical model of platelet aggregation in an extravascular injury under flow. Multiscale Model. Simul. 18, 1489–1524. http://dx.doi.org/10.1137/ 20M1317785, arXiv:2003.02251.
- Pabinger, I., Ay, C., 2009. Biomarkers and venous thromboembolism. Arterioscler. Thromb. Vasc. Biol. 29, 332–336. http://dx.doi.org/10.1161/ATVBAHA.108. 182188.
- Pivkin, I.V., Richardson, P.D., Karniadakis, G., 2006. Blood flow velocity effects and role of activation delay time on growth and form of platelet thrombi. Proc. Natl. Acad. Sci. USA 103. 17164–17169. http://dx.doi.org/10.1073/pnas.0608546103.
- Polasek, J., 2006. Three modes of platelet degranulation. Pathophysiol. Haemostasis Thromb. 35, 408–409. http://dx.doi.org/10.1159/000097698.
- Rana, A., Westein, E., Niego, B., Hagemeyer, C.E., 2019. Shear-dependent platelet aggregation: Mechanisms and therapeutic opportunities. Front. Cardiovasc. Med. 6, 1–21. http://dx.doi.org/10.3389/fcvm.2019.00141.
- Raskob, G., Angchaisuksiri, P., Blanco, A., Buller, H., Gallus, A., Hunt, B., Hylek, E., Kakkar, A., Konstantinides, S., McCumber, M., Ozaki, Y., Wendelboe, A., Weitz, J.I., 2014. Thrombosis a major contributor to global disease burden. Arterioscler. Thromb. Vasc. Biol. 34, 2363–2371. http://dx.doi.org/10.1161/ATVBAHA.114. 304488
- Ruf, A., Frojmovic, M.M., Patscheke, H., 1997. Platelet aggregation. In: Bruchhausen, F., Walter, U. (Eds.), Platelets and their Factors. Springer, p. 83.
- Schoeman, R.M., Rana, K., Danes, N., Lehmann, M., Di Paola, J.A., Fogelson, A.L., Leiderman, K., Neeves, K.B., 2017. A microfluidic model of hemostasis sensitive to platelet function and coagulation. Cell. Molecular Bioeng. 10, 3–15. http://dx.doi. org/10.1007/s12195-016-0469-0.
- Stalker, T.J., Newman, D.K., Ma, P., Wannemacher, K.M., Brass, L.F., 2012. Platelet signalling. Handb. Exp. Pharmaco. 210, 59–85. http://dx.doi.org/10.1007/978-3-642-29423-5.
- Strogatz, S., 1994. Nonlinear Dynamics and Chaos: With Applications to Physics, Biology, Chemistry, Engineering, vol. 32, Perseus Books, http://dx.doi.org/10.5860/choice.32-0994.
- van der Meijden, P.E.J., Heemskerk, J.W.M., 2019. Platelet biology and functions: new concepts and clinical perspectives. Nat. Rev. Cardiol. 16, 166–179. http://dx.doi.org/10.1038/s41569-018-0110-0.
- Wang, N.T., Fogelson, A.L., 1999. Computational methods for continuum models of platelet aggregation. J. Comput. Phys. 151, 649–675. http://dx.doi.org/10.1006/ jcph.1999.6212.
- Xu, Z., Chen, N., Kamocka, M.M., Rosen, E.D., Alber, M., 2008. A multiscale model of thrombus development. J. R. Soc. Interface 5, 705–722. http://dx.doi.org/10. 1098/rsif.2007.1202.